

# Transport of water and oxygen in epoxy-based coatings

Hossein Zargarnezhad <sup>a,\*</sup>, Parham Zarei <sup>b</sup>, Dennis Wong <sup>c</sup>, C.N. Catherine Lam <sup>c</sup>, Edouard Asselin

<sup>a</sup>

<sup>a</sup> The University of British Columbia, Department of Materials Engineering, 309-6350 Stores Road, Vancouver, BC V6T 1Z4, Canada

<sup>b</sup> The University of British Columbia, Department of Physics & Astronomy, 6224 Agricultural Road, Vancouver, BC V6T 1Z1, Canada

<sup>c</sup> Shawcor Ltd., 25 Bethridge Road, Toronto, ON, M9W 1M7, Canada

\*Corresponding author: [hossein.zargar@ubc.ca](mailto:hossein.zargar@ubc.ca) (H. Zargarnezhad)

## ABSTRACT

Epoxies are used in various industrial applications as corrosion barriers but quantitative time-dependent predictions of their ability to mitigate corrosion attack at the metal/coating interface remain elusive. Permeability data for water and oxygen through epoxy-based coatings are of particular interest because the coating's barrier performance in humid environments is directly related to how quickly these reactants get to the metal/coating interface. There is, however, an absence of literature data to explain oxygen transport within coatings in the presence of condensed water and its associated plasticization effects. We show that water is a dominant player in the barrier performance of epoxy coatings because it blocks the transport of other permeants. Through analysis of the sorption isotherms and empirical permeation data, we determined adjustable parameters that explain water vapor plasticization effects in fusion bonded epoxy (FBE) at 65°C. At this temperature, evolution of cavity formation and break-up of water clusters result in high mobility of water molecules inside the epoxy network. We also modeled oxygen transport through FBE in wet-state conditions based on time lag measurements, and with reported literature data on vapor and gas sorption in epoxy. In a mixed gas/vapor system, condensed water in FBE blocks

and/or significantly decreases gas permeation in the coating. If the service temperature is low (less than 40°C), water immobilizes the oxygen gas within microvoid regions in the glassy epoxy. Our experimental measurements, combined with Freeman's theoretical model for upper bound limits, showed that this water-induced blocking mechanism is sufficient to suppress corrosion reactions on the underlying substrate material. At 65°C and above, the synergistic effect of coating plasticization by water molecules and dissolution of oxygen in a mobile water phase results in significant gaseous transport. We applied mathematical models based on proven sorption and transport models to FBE free-standing films and derived adjustable parameters to quantitatively explain this competitive permeation. Our O<sub>2</sub> transport data show that, compared to the single-layer FBE, epoxy-based coatings with additional polyolefin layers can improve the barrier performance by deprivation of micropore channels for gas transport.

#### **KEYWORDS**

Fusion bonded epoxy, Gas transport, Competitive permeation, Epoxy coatings, Wet-state conditions.

#### **1. Introduction**

Epoxy-based coatings yield a dense polymeric network to shield the underlying metal from corrosive environments. Polar groups within the epoxy (e.g., hydroxyl, amino, etc.) generate hydrogen bonding between polymeric chains and also restrain segmental motion in the polymeric network [1]. Such bonding and segment mobilities are central to the solubility and diffusivity of penetrants, such as oxygen, within the polymeric structure. Nevertheless, they are not constant attributes during the service life of a coating system and may significantly change due to thermal degradation or polymer hydration. Thus, a quantitative assessment of an epoxy-based coating's barrier properties requires mass transport data for gases, such as oxygen, within a myriad of operational conditions, including variations in service temperature and moisture.

Water is a highly interactive permeant in glassy membranes in that it remarkably alters the dynamics of transport for other species [2]. For binary diffusion systems, we can make a reasonable estimate for the relative permeability (or selectivity) of gas pairs using the so-called “upper bound” theory [3]. This model confirms that the permeability process changes from solution-diffusion to Knudsen diffusion (i.e., free molecular flow) as the pore size increases in the polymer [4]. Yet, prediction of this transition is qualitative in the upper bound analysis [4] and, oftentimes, calculated transport properties poorly correlate with the in-service performance of the coating layer [5]. In an a priori defect-free coating system, mass transport mechanisms within the coating are the major driver of subsequent failures, which are often causally linked to underlying corrosion and/or coating disbondment. To analyze coating structures that are expected to perform well over many years of service, it is necessary to fully understand the transport behaviour of at least two common corrosive substances: water and oxygen. Because these substances are prone to competitive transport in epoxy-based barrier coatings, and because they may result in plasticization of a given coating, it is important to study how oxygen gas is transported in the presence of water – i.e. data on dry-state permeation of oxygen cannot account for real-world observations in wet environments.

It is well-known that the mobility of gaseous permeants within glassy polymers significantly declines upon water sorption [6]. This is because water has an extremely small kinetic diameter ( $d$ ) and high condensability ( $\epsilon/K$ )—e.g.,  $d_{H_2O} < d_{H_2}$  &  $(\epsilon/K)_{H_2O} \gg (\epsilon/K)_{O_2}$ —and can fill up the micropores in the polymer to a greater extent than other permeants [7]. Minelli and Sarti [8] showed that for various glassy polymers, diffusivity (and permeability) of a condensable permeant (like CO<sub>2</sub>) can be described using only two adjustable parameters, even in the presence of plasticization effects. These parameters are the diffusivity at infinite dilution and an empirical constant referred to as the plasticization coefficient ( $\beta$  in their study [8]). The latter parameter expresses the mobility factor as an exponential function of permeant concentration. In a recent study [9], we examined water vapor

transport across fusion-bonded epoxy (FBE) as a function of temperature, and showed that the water vapor permeation isotherm in a standard FBE (with glass transition temperature  $\leq 115^{\circ}\text{C}$ ) at  $65^{\circ}\text{C}$  is similar to polymers that experience significant plasticization (e.g., see data for polyethylmethacrylate in [8]). This finding indicates that the gas selectivity of a standard FBE in humid environments may become complicated and may experience substantial changes, even for species with a low affinity constant for sorption in the polymer (e.g., oxygen). Indeed, gas selectivity might exceed values suggested from the Freeman theoretical model for upper bound limits [3] for a system containing  $\text{H}_2\text{O}$  and  $\text{O}_2$ .

The permeation of gas and water is likely a primary driver for under-coating corrosion of metal infrastructure, such as pipes. The literature suggests that the initial step in developing corrosion under organic coatings is the adhesion loss due to water ingress at the coating/substrate interface [10]. The corrosion cell is then controlled by oxygen permeability and other coating attributes such as “wet adhesion” performance [11]. An optimal combination of transport and other performance properties such as adhesion is the key feature of epoxy-based coatings, including FBE and High-Performance Powder Coating (HPPC) [12], [13]. There is, however, an absence of high-accuracy measurements to verify purported qualities of these coating systems such as good adhesion and resistance to cathodic disbondment in long term service conditions. Likewise, the low oxygen permeability of epoxy polymeric structures is often cited in the literature concerned with corrosion performance [14]–[16]. Yet to our knowledge, there is no study on oxygen permeability of epoxy-based coatings in wet-state conditions, which are common in most applications of these coatings [17]. Since the permeability coefficient of water in FBE is high ( $10^{-13}$  mol/m-s-Pa at  $25^{\circ}\text{C}$  [9]) and transport of water-dissolved oxygen through the glassy coating is anticipated [18], we might expect dissolved oxygen transport. In addition, at high activities, water molecules tend to self-associate rather than interact with the polymeric chains [19]. The contribution of self-association of water molecules (i.e., clustering effects) to gas transport, however, is unclear. Accordingly, data to

correlate barrier performance of the coatings and corrosion of the underlying substrate are scant, especially after the water-induced plasticization.

We are interested in how oxygen transmits through commonly applied epoxy-based coatings in humid environments to induce corrosion of underlying infrastructure such as pipes. Thus, we examine epoxy-based coating films for water-dissolved oxygen permeation. We carried out a time-lag assessment to analyze the gas permeability across FBE and HPPC coating systems while water was present in the system. The dissolved gas permeation rate through water-saturated films was empirically determined according to water activities in the upstream gas phase. We also applied mathematical models developed for glassy polymers to quantify adjustable parameters of competitive sorption based on our previously reported water permeability data [9] and on sorption data available in the literature. Then, permeation of water and oxygen through coating layers was directly modeled and described according to sorption and diffusion concepts for competitive transport.

## **2. Experimental**

### **2.1. Coating film preparation**

Free-standing coating films with no macroscopic defects were investigated in this study. Sheets of powder coating materials, including FBE, topcoat polyethylene (PE), and HPPC, were supplied by Shawcor Ltd. The FBE coating is based on the diglycidyl ether of bisphenol A (DGEBA) and dicyandiamide (DDA) as the curing agent [20]. Its formulation also contains mineral agents such as wollastonite ( $\text{CaSiO}_3$ ), aluminum oxide, and anatase titanium oxide [21], [22]. HPPC is a monolithic coating structure consisting of an FBE primer, an adhesive polyolefin co-polymer and a topcoat PE layer; thicknesses of the layers are typically 175-250  $\mu\text{m}$ , 125-150  $\mu\text{m}$ , and 500-800  $\mu\text{m}$ , respectively. All free-standing films used in this study were applied by the manufacturer on an easy release Teflon substrate and peeled off after curing. To understand the transport behavior of

the multilayered HPPC, we also tested topcoat PE for oxygen permeability and included its data herein for comparison. All free-standing films (400  $\mu\text{m}$ , 750  $\mu\text{m}$ , and 1200  $\mu\text{m}$  thick on average for FBE, topcoat PE, and HPPC, respectively) were cut individually into disk shape specimens. Individual film thicknesses were determined through standard procedures [23]. All films were dried under vacuum at 22°C for three days [24]. To minimize any age dependent behavior, all coating samples were used within five days of drying [19].

## 2.2. Dissolved oxygen permeation

Dissolved oxygen (DO) permeability measurements were done with a constant volume dual-chamber apparatus (Fig. 1). A DO probe and Mettler Toledo FiveGo DO meter F4 were used to measure the DO concentration in the downstream aqueous side. We employed two experimental arrangements to carry out permeation tests (i.e., Fig. 1a and 1b). In the first, we used an upstream gas vessel (the left side of the coating film in Fig. 1a) to monitor the effect of moisture penetration on the gas permeation process. This arrangement enabled us to examine the extent of relative gas permeability for an in-service coating system. For example, the topcoat PE in the multilayered HPPC is directly exposed to atmospheric moisture in service conditions, and accordingly hydration of FBE primer is slower compared to standard FBE systems. Since the working temperature limit for the DO probe was 50°C, we used this test apparatus only for measurements at low temperatures (i.e., 25 and 40°C). In the second configuration, we applied the gas pressure on a water-containing upstream volume and set both faces of the testing membrane at the temperature of the experiment (Fig. 1b). We then kept the aqueous phase around the DO probe at a temperature less than the probe working limit. We refer to these two experimental setups (Fig. 1a and 1b) as the low-temperature and the high-temperature tests, respectively. For the high-temperature tests at 65°C, we adjusted the oxygen partial pressure incrementally between 0 and 100 kPa in the upstream volume and measured the gas permeation rate with respect to partial pressures of water and oxygen in the total feed pressure. For tests at 70 and 80°C, measurements were carried out for water activity of 0.5 (i.e., at oxygen partial pressures equal to vapor pressure

in the feed volume). Permeability data for all experiments were taken as an average of three measurements (at minimum) for each test condition.

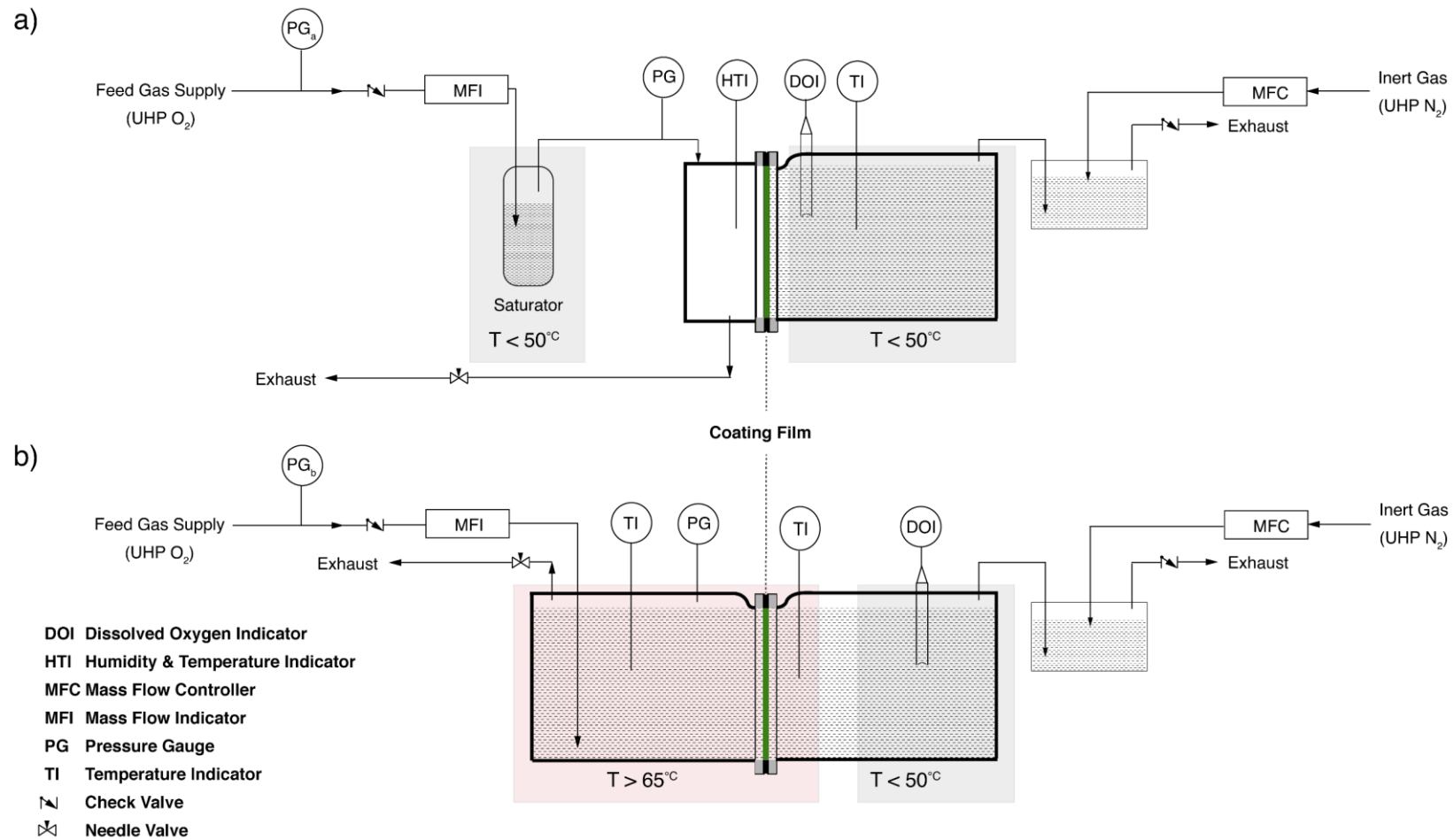


**Fig. 1.** Schematic of wet-state oxygen permeation apparatus for (a) the low- and (b) the high-temperature tests. In each arrangement, the pressure indicated by the pressure gauge is the sum of atmospheric pressure, water vapor saturation pressure in the upstream volume, and oxygen partial pressure. Hatched areas indicate liquid water in the shown volumes.

Let us recall that these experiments were carried out in such a way that the coating film was always in contact with liquid water. Since minor changes in partial pressure of water vapor (in the gaseous phase above water in each volume) across the sample result in insignificant water vapor transport, free-standing films were considered to be in equilibrium with condensed water after the initial water sorption stage in the experiments. Therefore, we did not monitor the condensed water transport in DO permeability measurements. However, we must note that water exists in both condensed and vapor phases within the glassy polymer [25]. Thus, we use vapor sorption data in epoxy based on the multilayer sorption theory for our mathematical modeling. Microstructural characterization of the FBE coating in the presence of water vapor has been discussed in detail elsewhere [9]. In all experiments, the downstream volume was connected to a relief compartment to maintain the total pressure of the gas phase in the downstream chamber at atmospheric pressure. Also, to ensure concentration polarization did not occur on either side of the testing membrane [26], the gas-water mixture was well-mixed at the surfaces of the coating film via an oxygen bubbler arrangement and a stirring magnet in the upstream and downstream volumes, respectively.

Prior to each test, nitrogen was allowed to flow through both sample chambers for 30 min at a slightly greater than atmospheric pressure to deaerate the water in contact with the coating membrane. The downstream vessel was then sealed against atmospheric air ingress and oxygen gas was applied in the upstream volume. Accordingly, boundary conditions for each test were as follows:

$$C(x, 0) = 0; \tag{1}$$

$$C(0, t) = C_0; \tag{2}$$

$$C(l, t) = C(t); \tag{3}$$

$C(x, t)$  being concentration of the oxygen gas (mg/L) at distance  $x$  (m) from the upstream face of the membrane at time  $t$  (s). The diffusion path is defined along the coating thickness ( $l$ ) starting from the coating surface in the upstream volume (i.e.,  $x = 0$ ).

The concentration of dissolved gas in the receiving volume was monitored and the transport capacity of the coating films was assessed through the solution of Fick's second law of diffusion. Detailed experimental procedures to analyze concentration rise in the downstream volume have been previously reported [27]. The permeability coefficient (mol/m-s-Pa) was defined as the product of the quantity of permeant and film thickness ( $l$ ) over the product of area ( $A$ ), time, and the pressure drop across the free-standing film. Therefore, using the equation of state for ideal gas, we applied the following equation to calculate permeability from the experimental results:

$$P = \left(\frac{dC}{dt}\right) \frac{Vl}{Ap_iRTK_H} \quad (4)$$

where  $dC/dt$  (mol/m<sup>3</sup>-s),  $V$  (m<sup>3</sup>),  $p_i$  (Pa),  $R$  (m<sup>3</sup>-Pa/K-mol),  $T$  (K), and  $K_H$  (mol/m<sup>3</sup>-Pa) are flux (or the rate of concentration increase at steady-state from experimental results), the volume above aqueous phase in the downstream, the pressure drop of oxygen across the sample, the universal gas constant, the test temperature and the Henry's law constant for O<sub>2</sub> dissolution in the downstream water, respectively. Values of  $K_H$  in Eq. (4) for different temperatures (< 50°C according to Fig. 1) were calculated from correlations for O<sub>2</sub> in H<sub>2</sub>O produced by Tromans [28]. Eq. (4) works well for single layer membranes such as FBE and topcoat PE. For the multilayered HPPC, however, standard procedures for thickness measurement were not applicable [9]. Therefore, consistent with the approach taken in our own earlier work [9], we used permeance (i.e.,  $P/l_{total}$ ) as the metric to assess the gas transport in HPPC.

Our experiments were run on 25 cm<sup>2</sup> films for which it is possible to measure permeability ( $P_{O_2}$ ) on the order of 10<sup>-14</sup> to 10<sup>-19</sup> mol/m-s-Pa (10<sup>-9</sup> to 10<sup>-14</sup> ccSTP/cm-s-cmHg) with the typical variation in film thickness (for the studied coatings) and partial pressure. This range provides the sufficient sensitivity to detect variations of O<sub>2</sub> permeability when it is in competition with water. Based on measurements reported for epoxy in dry conditions, oxygen permeability from 25 to 80°C is between 0.5×10<sup>-16</sup> and 2.5×10<sup>-16</sup> mol/m-s-Pa [12]. According to data reported in the literature [29], the minimum amount of oxygen necessary for corrosion of uncoated steel at atmospheric pressure

is 0.008 mg/cm<sup>2</sup>-d. This amount is equivalent to permeabilities of  $2.5 \times 10^{-16}$  and  $5.7 \times 10^{-16}$  mol/m-s-Pa for coating thicknesses between 200 and 400  $\mu\text{m}$ , respectively. Comparing these values with oxygen permeability data at dry conditions indicates that epoxy coatings at standard thicknesses ( $\sim 200 \mu\text{m}$  for HPPC and  $400 \mu\text{m}$  for FBE) can maintain the coating/metal interface well below the critical level for corrosion. While we note that the rate-determining role for corrosion of O<sub>2</sub> permeation through the coating to the substrate is still a matter of debate [11], we direct our attention to the consequences of ageing of the coating structure – e.g., an initial adhesion failure by formation of a crack-free blister. In fact, ingress of oxygen combined with other aggressive species generates more detrimental effects than under-coating corrosion and may equate more closely with O<sub>2</sub> permeability data. For example, oxygen concentration is critically important in cases of salt ingress into the coating/metal interface and at high salt concentrations, oxygen transmission through the coating becomes the controlling factor for corrosion [11].

### 3. Model equations

#### 3.1. H<sub>2</sub>O/O<sub>2</sub> upper bound relationship at ambient temperatures

A large body of experimental data on gas separation membranes suggests that there is a distinct trade-off relationship between permselectivity of the polymer for gas A over gas B,  $\alpha_{AB}$  ( $= P_A/P_B$ ), and permeability of the faster permeating gas ( $P_A$ ) for binary gas pairs. The collection of numerous empirical data by Robeson [30] showed that an upper bound to this relationship can be defined by a straight line on a log-log plot of  $\alpha_{AB}$  versus  $P_A$ . Freeman developed a theoretical model that defines this upper bound as a natural consequence of the strong size-sieving nature of the stiff chain glassy polymers [3], where  $\alpha_{AB} = \beta_{AB}/P_A^{\lambda_{AB}}$ . He defined the exponential component based on the reduced kinetic diameter as  $\lambda_{AB} = (d_B/d_A)^2 - 1$ ,  $d_i$  being the kinetic diameter (in units of m) of gas pairs. He also derived an empirical expression for the coefficient component,  $\beta_{AB}$ , based on  $\lambda_{AB}$  and a solubility selectivity term which directly correlates with condensability parameters of

gases and polymer type of interest (i.e., rubbery or glassy). These parameters are identified as follows [30]:

$$\beta_{AB} = \frac{S_A}{S_B} S_i^{\lambda_{AB}} \exp \left[ -\lambda_{AB} \left( b - f \frac{1-a}{RT} \right) \right] \quad (5)$$

$$\ln S = M + N(T_x) \quad (6)$$

where  $S$  and  $T_x$  are solubility (mol/Pa·m<sup>3</sup>) and a condensability measure (e.g., critical temperature or  $\varepsilon/k$  in units of K) of gas A or B, respectively. In Eq. (5),  $a$ ,  $b$ , and  $f$  are adjustable parameters with values of 0.64, 11.5 cm<sup>2</sup>/s (for glassy polymers), and 12,600 cal/mol, respectively.  $M$  and  $N$  in Eq. (6) are also –6.91 cm<sup>3</sup>(STP)/(cc·cmHg) and 0.0153, respectively.  $M$  and  $N$  are strongly affected by the applied gas pressure and a deviation from the "upper bound" behavior is likely when gas sorption in the polymer is pressure dependent [31]. For approximating the empirical upper bound relationship, Robeson utilized studies listing permeability data for light gas pairs (e.g., H<sub>2</sub>/O<sub>2</sub>, H<sub>2</sub>/N<sub>2</sub>) in various polymers. That being said, the upper bound observation has also been shown to be applicable for wet gas mixtures (e.g., H<sub>2</sub>O/CO<sub>2</sub> gas pair in [19]).

The upper bound theory enables us to determine the minimum gas permeability through a glassy polymeric coating in a humid gas mixture from its water permeability coefficient ( $P_w$ , mol/m·s·Pa) [3]. Alternatively stated, the upper bound theory shows that amorphous polymeric structures with high glass transition temperature, rigid backbone, and relatively high fractional free volume lie on or near the Robeson plot line [3]. Thus, applying this theory gives us a means to evaluate water/gas permeability trade-offs in glassy polymers. Thus, we used the Freeman theoretical model to estimate the epoxy coatings' performance prior to initiation of water-induced plasticization effects (i.e., < 65°C [9]).

### 3.2. Models developed for competitive permeation at elevated temperatures

The water sorption process becomes dominated by self-association mechanisms with rising water activity and temperature [32]. The resultant water clustering decreases the fractional free volume and increases plasticization in a glassy polymer [33], [34]. Since correlations between permeability,

diffusivity and solubility often employ the fractional free volume in a polymer, it is reasonable to assume that new sorption sites are less available to larger gas molecules after hydration [31]. There are a few good modelling descriptions for the onset of plasticization and its effect on competitive gas sorption [35], [36]. These models usually consider the dual mode sorption (DMS) behavior of gases in glassy polymers to explain competitive permeation of gases in mixed conditions [37]. Gas molecules are either absorbed directly into the polymer matrix (i.e., Henry's law region shown as  $C_{DA}$ ) or adsorbed into micro-cavities within the matrix (i.e., Langmuir adsorption shown as  $C_{HA}$ ):

$$C_A = C_{DA} + C_{HA} = k_{DA}f_A + \frac{C'_{HA}b'_A f_A}{1 + b'_A f_A} \quad (7)$$

where  $k_{DA}$ ,  $C'_{HA}$ ,  $b'_A$  and  $f_i$  are Henry's law constant (for solubility of gas A in polymer in mol/m<sup>3</sup>-Pa), maximum gas concentration (mol/m<sup>3</sup> polymer), Langmuir affinity constant (Pa<sup>-1</sup>) and the fugacity (Pa) of the gaseous penetrant A. In multi-component systems, it is only the Langmuir sorption sites that are involved in competitive sorption: a second term (i.e.,  $b'_B f_B$  for gas B) is added in the denominator of the Langmuir sorption term in Eq. (7) [38]. Although the DMS model provides a rigorous approximation for the gas sorption process, it cannot reflect the effect of strong polymer-vapor and vapor-vapor interactions, especially at high vapor pressures [7]. Feng [25] showed that for a condensable vapor (at fugacity of  $f_w$ ), a modified DMS model can better describe vapor sorption isotherms that include water vapor clustering:

$$C = \frac{\bar{C}_p k' f_w / f_0}{1 - k' f_w / f_0} + \frac{\bar{C}_p (A' - 1) k' f_w / f_0}{1 + (A' - 1) k' f_w / f_0} \quad (8)$$

where  $\bar{C}_p$  is the weighted mean sorption capacity for a monolayer of penetrant (mol/m<sup>3</sup> polymer),  $k'$  indicates the interaction between the vapor molecule and the polymer molecular segment,  $f_0$  is the saturated vapor fugacity (Pa) at the measurement temperature and  $A'$  measures the interaction of the vapor molecule and the microvoids. In Eq. (8), the microvoid affinity constant in the DMS model is essentially redefined as follows:

$$b'_w = \frac{(A' - 1)k'}{f_0} \quad (9)$$

In fact, we can determine sorption parameters for water vapor (i.e., adjustable coefficients in Eq. (8)) in a glassy polymer by fitting data from vapor sorption experiments to this equation [36]. Since the vapor transport properties of FBE agree reasonably well with published data for other epoxy formulations [9], we applied Eq. (8) and solubility data from the literature [39] for epoxy to determine the modified DMS parameters.

For analyzing diffusivity and permeability, Chen et al. [40] showed that the diffusion coefficient of simple gases in a system containing water vapor cannot be a constant value. That is because, in a humid feed gas, the interference of water vapor molecules, or clusters thereof, with the diffusional pathways for gaseous species is extremely likely. These workers assumed that the changes in the gas diffusivity are exponentially dependent upon the mobile concentration of water vapor ( $C_{mw}$ ):

$$D_A = D_{A,0} \exp(\beta' C_{mw}) \quad (10)$$

where  $D_{A,0}$  (m<sup>2</sup>/s) is the diffusion coefficient in the limit of zero vapor concentration.  $\beta'$  (m<sup>3</sup>/mol) also accounts for plasticizing ability of the wet mixture (i.e., water vapor and penetrant A) and is specific to water vapor and other plasticizing permeants (e.g., CO<sub>2</sub>) [40]. A positive value of  $\beta'$  is indicative of plasticization (swelling), while its negative values contributes to anti-plasticization (blocking) behavior and reduction of diffusivity with increasing humidity [41]. For several glassy polymers, water vapor appears to cause both plasticization and anti-plasticization and this behavior can change with temperature [42]. Scholes et al. [36] showed we can derive an equation for the steady-state permeability of water using Eq. (10) to calculate the flux for vapor transport thus:

$$\bar{P}_w = \frac{D_{w,0}}{\beta'_w(f_{w2} - f_{w1})} \left\{ \exp \left[ \beta'_w \left( \frac{\bar{C}_p k' f_{w2}/f_0}{1 - k' f_{w2}/f_0} + \frac{F_w \bar{C}_p b'_w f_{w2}}{1 + b'_w f_{w2}} \right) \right] - \exp \left[ \beta'_w \left( \frac{\bar{C}_p k' f_{w1}/f_0}{1 - k' f_{w1}/f_0} + \frac{F_w \bar{C}_p b'_w f_{w1}}{1 + b'_w f_{w1}} \right) \right] \right\} \quad (11)$$

where  $F$  is the immobilization factor, a coefficient between zero and unity, which denotes the mobile fraction of the gas/vapor dissolved in Langmuir domains. Subscripts w, 2, and 1 also denote values associated with water, the upstream, and downstream conditions, respectively. We revisited our

earlier experimental report for water transport in FBE [9] and employed Eq. (11) to estimate the infinite dilution diffusivity ( $D_{w,0}$ , m<sup>2</sup>/s), the immobilization factor ( $F_w$ ), and the plasticization potential ( $\beta'_w$ , mol/m<sup>3</sup>) of water vapor.

For a system containing gas (A) mixed with water vapor, the gas diffusivity is also exponentially dependent upon the mobile concentration of water:  $D_{A,wet} = D_A \exp(\beta'_{w-A} C_{mw})$  [36], [43]. This yields the steady-state permeability of the gaseous component ( $\bar{P}_A$ ) [40]:

$$\bar{P}_A = \frac{D_A}{f_{A2} - f_{A1}} \left\{ \exp \left[ \beta'_{w-A} \left( \frac{\bar{C}_p k' f_{w2}/f_0}{1 - k' f_{w2}/f_0} + \frac{F_w \bar{C}_p b'_w f_{w2}}{1 + b'_A f_{A2} + b'_w f_{w2}} \right) \right] \left( k_{DA} + \frac{F_A C_{HA} b'_A}{1 + b'_A f_{A2} + b'_w f_{w2}} \right) f_{A2} \right. \\ \left. - \exp \left[ \beta'_{w-A} \left( \frac{\bar{C}_p k' f_{w1}/f_0}{1 - k' f_{w1}/f_0} + \frac{F_w \bar{C}_p b'_w f_{w1}}{1 + b'_A f_{A1} + b'_w f_{w1}} \right) \right] \left( k_{DA} + \frac{F_A C_{HA} b'_A}{1 + b'_A f_{A1} + b'_w f_{w1}} \right) f_{A1} \right\} \quad (12)$$

Using empirical data from dissolved oxygen transport permeation, we can apply Eq. (12) to determine associated immobilization factor ( $F_A$ ) and plasticization potential ( $\beta'_{w-O_2}$ ) in FBE. Modeling of all experimental data in this work was undertaken using a nonlinear regression approach based on a maximum likelihood estimation algorithm developed in MATLAB R2021a.

#### 4. Single permeant solubility in epoxy

##### 4.1. Water

In order to understand the fundamentals of gas transport in the coating under humid conditions, pressure-dependent sorption data for epoxy was required. Previously reported water sorption isotherms of epoxy systems with compositions similar to FBE [39] have been used in this work and fitted to the mathematical models discussed above to generate data for experimental temperatures of interest. Empirical studies on epoxy materials show that no substantial contrast exists between DGEBA epoxy systems in water sorption characteristics when different curing agents are used, and it is only the polymer resin that is involved in the water diffusion process [39], [44]. Thus, we used pressure-dependent sorption data of DGEBA/DAMP epoxy system published by Lacombe

et al. [39] to obtain the modified DMS parameters for H<sub>2</sub>O in FBE. A detailed description of water sorption isotherm calculations at elevated temperatures is included in Appendix A. The modified DMS parameters are summarized in Table 1.

**Table 1**

Estimated values for weighted mean sorption capacity ( $\bar{C}_p$ ), and water sorption parameters ( $A'$  and  $k'$ ) using the modified dual-mode sorption model (Eq. (8)) and literature data [39]. The water Langmuir affinity constant ( $b'_w$ ) is determined from Eq. (9).

Temperature (°C)	65 <sup>a</sup>	70	80
$\bar{C}_p$ , mol/m <sup>3</sup>	694	674	622
$A'$ , –	3.754	3.753	3.753
$k'$ , –	0.601	0.601	0.601
$b'_w$ , ( $\times 10^{-5}$ ) Pa <sup>-1</sup>	6.61	5.31	3.49

<sup>a</sup> Estimations for all temperatures were based on data from [39] for 50°C and equations in Appendix A.

Fig. 2 shows the water concentration within the epoxy as a function of water activity in the polymer (i.e.,  $f_w/f_0$ ) and temperature according to the obtained modified DMS model parameters listed in Table 1. Based on empirical data from Lacombe et al. [39] (shown in the insert of Fig. 2), water clustering effects in epoxy (i.e., the inflection point in sorption isotherms) appear at temperatures lower than 45°C. While this temperature is the threshold temperature for cluster formation based on the Flory-Huggins theory [45], empirical studies on epoxy systems show that long-term ageing can also cause a similar sorption type below 45°C [46]. In addition, sorption curves in Fig. 2 reveal that deviation from Henry's type sorption in epoxy occurs around a water activity of 0.6 (i.e., 60% of the saturation pressure of water). This fact suggests that water can effectively hydrate the epoxy and become the dominant solute in the polymeric network at pressures over about half of the vapor saturation pressure. Upon further water sorption, dissolved vapor molecules form an ordered

structure (i.e., self-association) that decreases the diffusivity inside the polymeric network [9], [19]. In other words, the onset of clustering establishes competitive transport in water/gas mixtures.

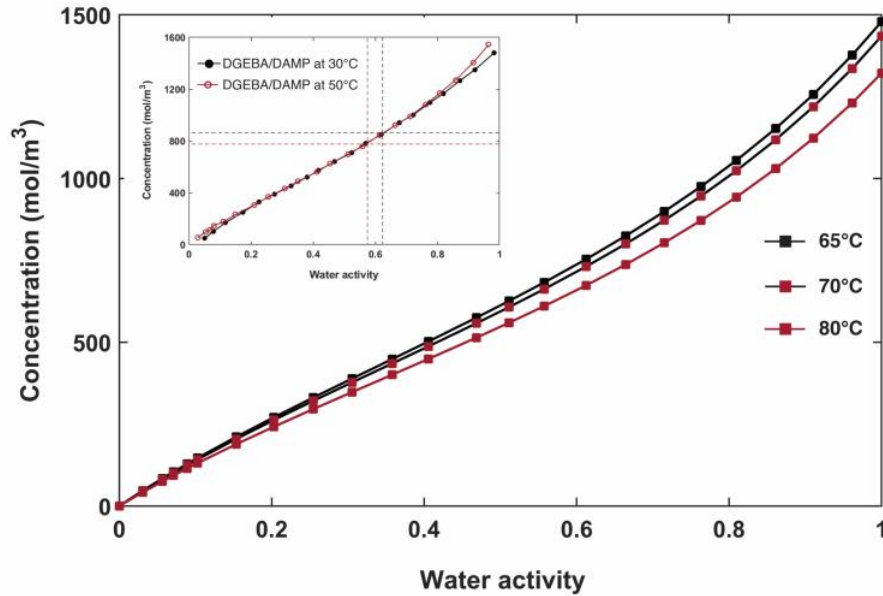


**Fig. 2.** Water sorption expressed as concentration ( $\text{mol/m}^3$ ) in epoxy materials similar to fusion bonded epoxy as a function of water activity in the polymer and temperature, based on fitting experimental data from [39] to Eq. (8). Water activity is equilibrium water vapor concentration inside the polymer ( $f_w$ ) over equilibrium water vapor pressure ( $f_0$ ) at the temperature of interest. Inset: experimental sorption data for DGEBA/DAMP epoxy at 30 and 50°C [39]; dashed lines show the inflection points from Henry's type sorption. Copyright 2018. Reproduced from [92] with permission from Springer US.

We used data from a DGEBA/DAMP epoxy at 50°C in [39] to generate sigmoidal isotherms for 65 to 80 °C through Eq. (8), which were required for permeation analyses – i.e., Eq. (11) and (12). For temperatures lower than this limit, one may directly use the experimental data and apply Eq. (7) for sorption analysis. According to Fig. 2, increasing temperature reduces the amount of water vapor sorbed into epoxy. The water interactions with the microvoid regions ( $A'$ ) and polymer matrix ( $k'$ ) do not vary significantly with temperature and it is the weighted mean sorption capacity ( $\overline{C_p}$ )

that shows a meaningful effect for temperature on water sorption (Table 1). In fact, the capacity of the polymeric network to sorb water in the first monolayer decreases with temperature, which is a characteristic behavior of physisorption processes [36].

We presented water vapor permeabilities for FBE at 65°C under variable feed conditions in our earlier work [9] (as shown in the insert of Fig. 3) and using a Brute-force integration method over average permeability data, we derived curves that represent the spot permeability for water transport at 65°C. Here, consistent with the approach taken by Chen et al. [40], we applied Eq. (11) to data from the spot permeability curve for wet-cup data, which is compatible with test conditions in oxygen permeation tests, and determined empirical constants for water transport in epoxy. Again, we should note that for permeability analyses, water activity parameter is used to refer to vapor concentration in the feed gas mixture (i.e., vapor pressure over the total pressure in the upstream volume). Within experimental error (~ 5% of the measured values), the new calculated permeability plot fitted reasonably well with values extracted directly from experimental data. Fitting results including the infinitely dilute Fickian diffusion coefficient ( $D_{w0}$ , m<sup>2</sup>/s), immobilization factor ( $F_w$ ), and the exponential concentration dependent factor ( $\beta'_w$  or plasticization potential of water, mol/m<sup>3</sup>) were provided in Table 2.

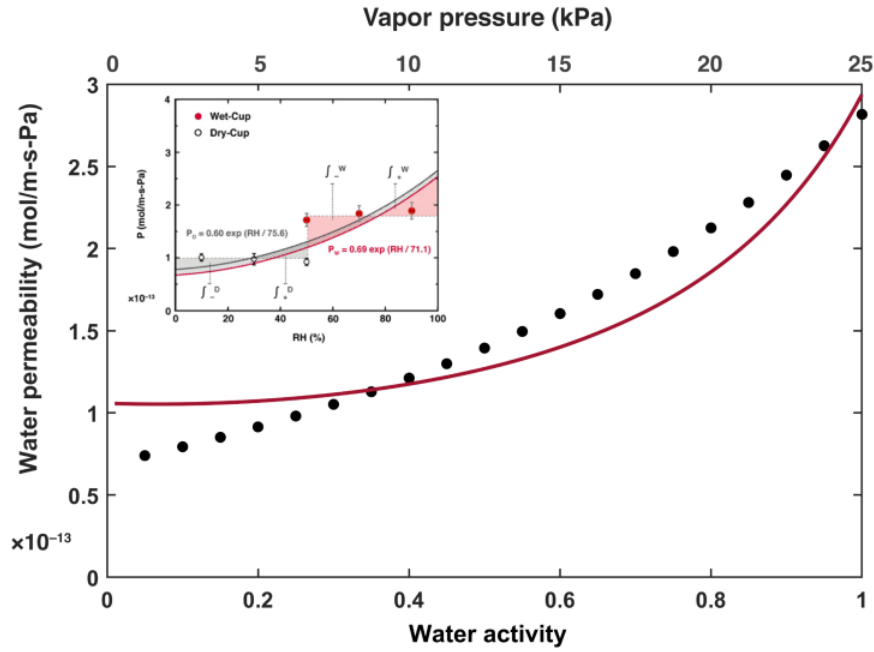


**Fig. 3.** Water vapor permeability (mol/m-s-Pa) in fusion bonded epoxy as a function of water activity in the upstream feed, at 65°C. Black markers (●) indicate the spot permeability curve for wet-cup data from our water permeation analysis (reported previously [9]) and the solid line represents the model fit to Eq. (11). Inset: average water vapor permeability data versus relative humidity from cup method measurements on fusion bonded epoxy at 65°C and derivation of spot permeability curves using a Brute-force integration analysis. Copyright 2022. Reproduced from [9] with permission from Elsevier Ltd.

**Table 2**

H<sub>2</sub>O permeability model parameters for FBE at 65°C, determined from Eq. (11).

	$D_{w,0}$ , (m <sup>2</sup> /s)	$\beta'_w$ , (mol/m <sup>3</sup> )	$F_w$ , –
FBE at 65°C	$2.68 \times 10^{-12}$	0.0011	0.49

The infinitely dilute Fickian diffusion coefficient ( $D_{w,0}$ ) in Table 2 is within the range of values found in the literature for water in epoxy resins [1], [7], [47]. Our earlier work on FBE [9] and that of other

workers on glassy polymers ([2], [19], [40]) suggest that the increasing permeability observed as water activity increases, for a given temperature, is a result of increasing water solubility in the polymer. Upon the formation of water clusters, we may expect a decrease in diffusivity within the polymer due to self-association of vapor molecules [48]. Having said that, the estimated water immobilization factor ( $F_w = 0.49$ ) for FBE implies that nearly half of the micro-voids in FBE contribute to the vapor permeance. This is in part related to the break-up of water vapor clusters within FBE at temperatures around 65°C and suggests that almost half of the microvoid regions within epoxy are actively contributing to vapor transport and, thus, cannot be considered dead ends. Another explanation for this value for immobilization factor could be cavity formations in the epoxy resin due to hygrothermal exposure which increases connectivity between microvoid domains throughout the FBE membrane [9]. This makes the microvoid channels in the coating more accessible for diffusive transport. In addition, the positive value of the plasticization potential is another quantitative metric for the extent of swelling in FBE due to hydrothermal exposure. The plasticization potential obtained here is remarkably smaller than that of high free volume polymeric membranes [36]. This small value is, however, of significance since it contributes to the corrosion barrier performance of the coating system. This constant is specific to water vapor transport and may not be applicable for competitive permeation processes [40] – i.e.,  $\beta'_w \neq \beta'_{w-A}$ .

#### 4.2. Oxygen

Literature data on oxygen solubility into epoxy systems are scarce. A major complication in characterization of O<sub>2</sub> transfer through glassy polymers is the chemical oxidation of the epoxy network during measurements, particularly at elevated temperature [49]. The uncertainty in the yield data can become more pronounced when thick films (above ~100–200 μm) are used [12]. There is, however, some evidence showing that plasticization and swelling effects are minimal for oxygen partial pressures below 1 atm and, thus, Henry's law can be used to calculate oxygen fugacity in epoxy based materials [12]. This has been verified experimentally for polyimides with comparable O<sub>2</sub> permeability, diffusivity, and solubility to epoxies and an excellent linearity of

permeability vs.  $O_2$  partial pressure supports negligible involvement of microvoids in  $O_2$  sorption [12]. Thus, to minimize the number of fitting parameters in the model, we approximated  $C_A$  with  $C_{HA}$  for  $O_2$  in the DMS model (Eq. (7)) and assumed that the immobilization factor for  $O_2$  is negligible in Eq. (12) ( $F_{O_2} \approx 0$ ).

## 5. Competitive transport in epoxy coatings

### 5.1. Analysis for the low-temperature tests (25 and 40°C)

Oxygen transport through the FBE film at low temperatures (i.e., 25 and 40°C) was strongly affected by water sorption. The lack of any measurable gas flux over 10 days suggested that FBE blocks oxygen transport in the presence of condensed water inside the polymeric network (Fig. 4). On the contrary, topcoat PE films showed equilibrium fluxes of the permeating gas in similar conditions, which nearly matched with the literature data for HDPE [7]. Detailed discussions for the general downstream concentration plot for DO (i.e., the initial pseudo-steady-state, followed by a linear flux) have been presented elsewhere [27]. The FBE film in contact with water did not show a steady-state flux of oxygen gas at these temperatures and the downstream concentration remained in plateau for upstream pressures of common interest (i.e., oxygen partial pressures up to 100kPa). To ensure this result was not limited to the specific boundary conditions in Fig. 1a, we also carried out several tests using the arrangement in Fig. 1b (i.e., aqueous upstream and downstream volumes). Again, a similar plateau confirmed the blocking mechanism in the low-temperature tests. This finding is perhaps not surprising since the dominant parameter in gas permeation is its mobility in diffusional pathways, which are the domains occupied by water molecules in the system under study [50]. The initial increase in downstream volume for FBE was primarily because the hydrated epoxy film had less fractional free volume than the initially-dry film, and once the water sorption occurred, gas immobilization began.

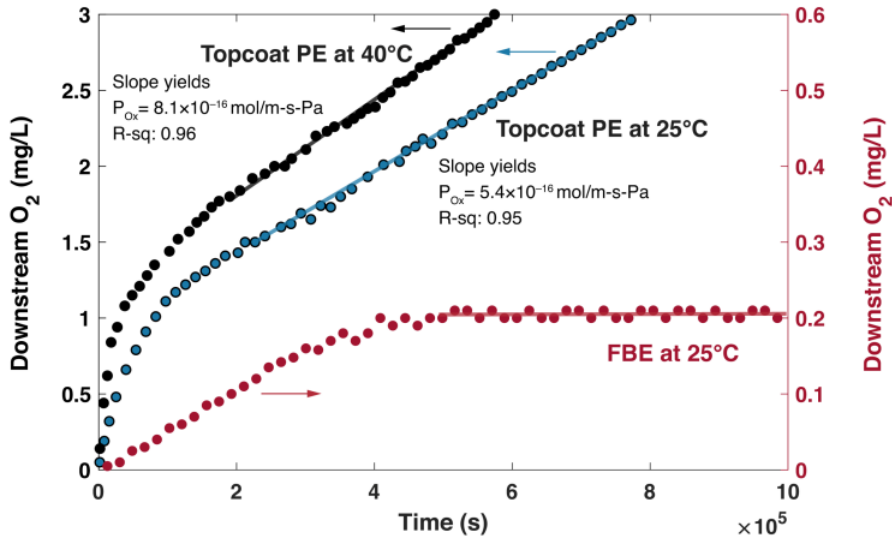


**Fig. 4.** Changes in downstream dissolved oxygen using topcoat polyethylene and fusion bonded epoxy at ambient temperatures (based on measurements by the test apparatus shown in Fig. 1a with  $O_2$  partial pressure of 20 kPa).

According to the Paul and Koros theory of immobilization [38], one can expect a constant permeability and a very pressure-dependent time lag if total immobilization occurs in glassy polymers. On the other hand, an increase in upstream gas pressure has a slight decreasing effect on gas permeability and the diffusion time lag only when there is incomplete immobilization of the gas held by the Langmuir sites [38]. As shown in Fig. 5, our time lag measurements at different upstream pressures revealed that the latter case was in better agreement with a hydrated epoxy membrane. According to Fig. 5, detection of oxygen permeability was possible at the oxygen partial pressure of 15 kPa in the upstream side. However, a similar test at  $p_{O_2} = 20$  kPa decreased the permeative flux and reduced the  $O_2$  permeability. We should note that the repeatability of the experimental determination of the  $O_2$  permeability coefficient was challenging at these boundary conditions. Both experiments shown in Fig. 5 reached a plateau over longer timescales. Similar issues have been addressed in the literature focused on oxygen permeation in epoxy systems [51]. Celina and Quintana [12] also showed that for relatively thick epoxy test specimens (around 500

μm), oxygen loss due to chemical reaction with the polymer (i.e., oxidation) is significant and determination of permeability would become complicated.

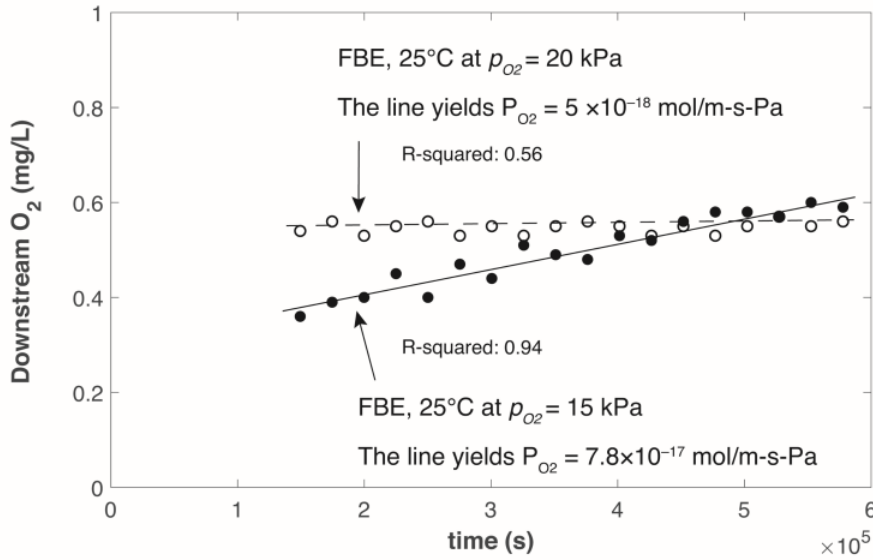


**Fig. 5.** Evolution of dissolved oxygen in downstream volume using fusion bonded epoxy at 25°C and low partial pressures of O<sub>2</sub> in the upstream side. Calculations are only based on slope of concentration vs. time before reaching the steady state plateau and the resulting permeability values represent transient transport rates.

It is indeed the trade-off between water sorption and gas mobility that regulates the gas transport in a mixed system. The Freeman theory of upper bound relationships [3] suggests a minimum permeability for the less permeable gas based on the kinetic diameters of the respective gas pair. Table 3 includes values of transport data for a glassy polymer at limits within our low-temperature tests based on upper bound relationships for water and oxygen. Calculations of transport data here were based on the average solubility coefficients correlated with critical temperature of water and oxygen in Eq. (6). We employed critical temperature in this work because results for water sorption were in a better agreement with the experimental database for epoxy than those from gas condensability or boiling temperature, which also represent  $T_x$  in Eq. (6) [31].

**Table 3**

Estimation of transport data for glassy polymers for a system containing water/oxygen mixture based on the upper bound theory

Temperature (°C)	$S_{H_2O}^a$ (mol/m <sup>3</sup> -Pa)	Theoretical $S_{O_2}$ $\times 10^4$ (mol/m <sup>3</sup> -Pa)	$\beta_{H_2O/O_2}$ (-)	Theoretical $\alpha_{H_2O/O_2}$ $\times 10^{-10}$ (-)	Theoretical $P_{O_2}$ $\times 10^{24}$ (mol/m-s-Pa)
25	0.668	3.56	94.23	13.70	0.73
40	0.253	3.00	16.51	1.58	11.4

<sup>a</sup> Values are comparable to those reported in the literature for epoxy systems [52]

Data presented in Table 3 indicate a dominant effect of water on O<sub>2</sub> transport in high-performance polymeric coatings. It is likely that FBE is a less selective membrane for oxygen than the limits suggested by the Freeman theoretical model. However, the data still provide an order of magnitude comparison for steady-state gas permeation, at least for temperatures where the polymer can retain its chain stiffness (i.e., < 65°C [9]). This analysis and our O<sub>2</sub> permeability measurements reveal that the hydrated FBE has good barrier performance against gas ingress in humid conditions. Accordingly, we expect appreciably less oxygen transport ( $1 \times 10^{-11} < O_2 \text{ flux} < 1.35 \times 10^{-6} \text{ mg/cm}^2\text{-d}$ ) across the FBE coating as compared to dry-state permeation. Thus, unless the moisture content of FBE is decreased to less than half of the solubility in saturated conditions, which then facilitates the gas mobility, the corrosion cell underneath the coating at low temperatures is less likely to be completed by oxygen in wet environments. This shows that oxygen supply is the rate-determining step for the under-coating corrosion reaction at temperatures less than 45°C in humid environments. Also, since plasticization by water is minimal at these temperatures, it is likely that the system reaches an equilibrium state upon the initial moisture uptake and maintains its barrier protection, at least in absence of external stimuli such as mechanical stress.

The multilayered HPPC also had a gradual decrease of oxygen flux over time (Fig. 6). Let us recall that for HPPC specimens, the gas permeation was measured with the downstream water exposed to the topcoat PE face of the coating. Since the PE component in HPPC is an effective barrier against water transmission (and also a relatively poor protection for gas ingress), O<sub>2</sub> transport experienced an extended two-stage sorption compared to FBE: a gradual increase, followed by a plateau upon saturation of the FBE primer. The gaseous flux through HPPC initiated at a maximum rate, gradually decreased upon vapor transport through the PE layer, and eventually reached a plateau. In fact, water tends to form clusters in the microvoids within the epoxy primer and this is sufficient to occupy and block the gas transport in the coating system. Again, results for O<sub>2</sub> permeation at 25°C and 40°C were similar, except that the time for reaching the saturation in FBE primer was shorter for HPPC specimens tested at 40°C (due to the higher vapor transmission rate through the topcoat PE).

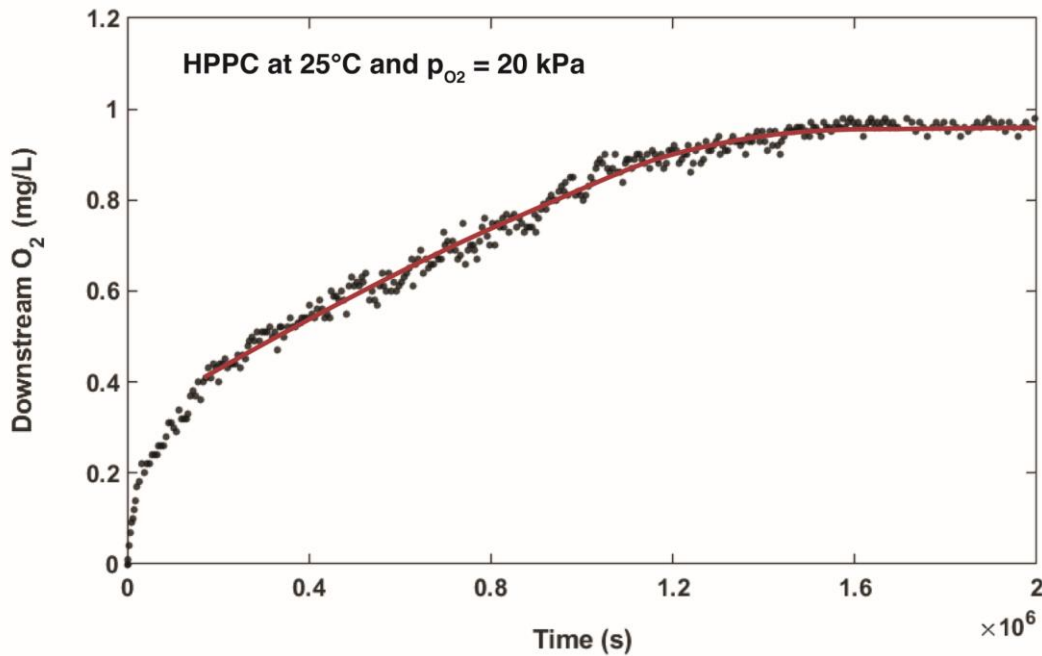


**Fig. 6.** Downstream dissolved oxygen as a function of time using the high-performance powder coating film at 25°C. The solid red line is for guidance only.

## 5.2. Coating performance at 65 to 80°C

Once self-association of water molecules is kinetically favored in the system (i.e., at temperatures slightly above 45°C), water diffusivity decreases and involvement of microvoids in gas transport changes the barrier performance [9]. Thus, water clustering and microvoid formation affect the mobile concentration of water in the FBE film, resulting in slight changes in gas permeability under humidified conditions (Eq. (10)) [40]. Our observations for O<sub>2</sub> permeation in FBE at 65°C (using the test apparatus in Fig. 1b) were non-negligible steady-state fluxes (i.e., similar to those of topcoat PE in Fig. 4). Values of O<sub>2</sub> permeability for FBE at 65°C with a feed of variable humidity are provided in Fig. 7. It should be noted that at higher water activities, above 0.5, achieving a steady-state permeability was challenging. An explanation for this difficulty was the high feed flowrates of oxygen in the upstream volume necessary to avoid concentration polarization in the experiment, which caused quick evaporation of the water within the upstream chamber. This issue, which was manifested in large error bars in permeability data, has been addressed in prior work in the literature for gas and water vapor transport in high free volume membranes [36]. Wet-state oxygen permeation data in Fig. 7 indicate that we might expect a gradual decrease in O<sub>2</sub> permeability with increasing water activity in the upstream gaseous volume. As has been shown in Fig. 7, values obtained here for permeability in wet conditions were significantly smaller than those of measurements in the absence of moisture (based on previous work in literature [12]). This shows that oxygen transport through the glassy epoxy drops considerably in humid environments, perhaps as a result of hydrolytic degradation during high temperature exposure [12]. The extent of blocking behavior in FBE at high vapor activities in the upstream feed volume was high and the oxygen gas flux (e.g., at  $a_w > 0.7$ ) resulted in permeabilities lower than  $10^{-19}$  mol/m-s-Pa (i.e., our detection limit). Having said that, the water-induced blocking seemed less effective compared to that observed at lower temperatures. Unlike the low-temperature tests, we observed an increase in the gaseous flux at higher partial pressures of oxygen in the upstream volume. This did not come as a surprise since the low chain stiffness in the polymeric structure due to the rise in temperature can induce a reduction in gas selectivity in humid environments [19]. However, to reach a

satisfactory description of the general behaviors observed, we applied the literature-proven transport models to analyze O<sub>2</sub> permeability in FBE.

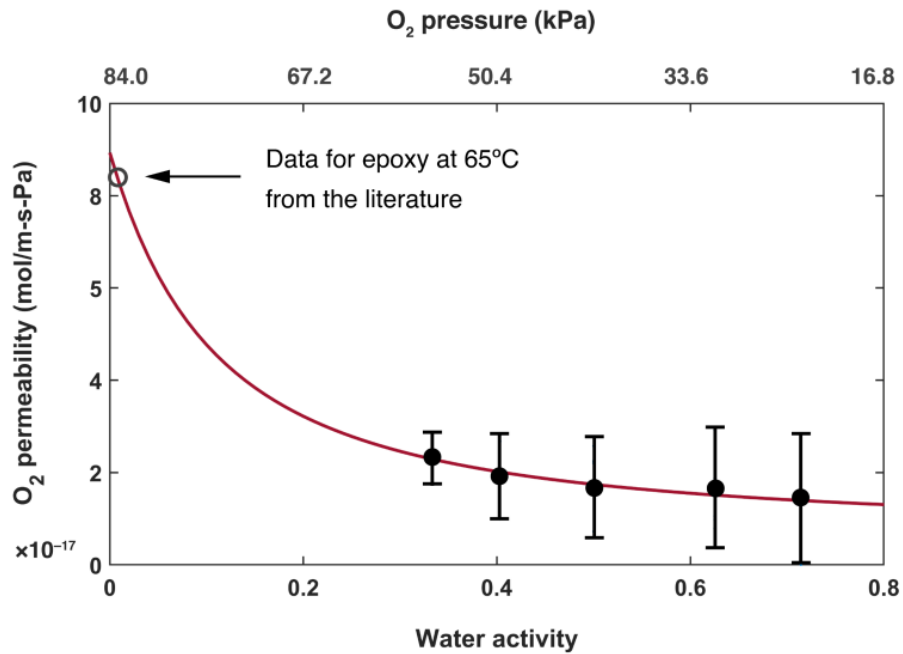


**Fig. 7.** Permeability of oxygen at different water activities for fusion bonded epoxy at 65°C. Copyright 2018. Literature data were adapted from [12] with permission from Elsevier Ltd. Here, water activity is the equilibrium water vapor pressure over the total pressure (water vapor + oxygen) in upstream feed volume.

The competitive sorption and plasticization effects were directly modeled through Eq. (12), with the fitted parameters listed in Table 4. For this analysis, we used experimental results from our own wet-state permeation measurements and the literature reported data on oxygen permeability coefficient in dry-state for epoxy materials similar to FBE [12]. Our mathematical modeling showed that not only did the water sorption dominate the gas transport, but it also had a major influence on oxygen sorption parameters in Eq. (12). Although little data are available for O<sub>2</sub> sorption in epoxy, literature reports on glassy polymers show that the Henry's law constant for oxygen sorption in dry-gas streams are significantly lower than our estimated  $k_{D,O_2}$ — e.g.,  $5.2 \times 10^{-5}$  mol/m<sup>3</sup>-Pa for

Epon828/A2049 at 65°C in [12] or data for other glassy polymers in [53]. In fact, this coefficient is correlated with the condensability parameter ( $\varepsilon/k$  in units of K) of the permeating gas [54]:

$$k_D = k_{D0} e^{m\varepsilon/kT} \quad (13)$$

where T denotes temperature (K) and m is a constant parameter ( $\sim 6.67 \pm 0.5$ ) and is independent of the penetrant or the nature of the polymeric phase. In Eq. (13),  $k_{D0}$  is a function of permeable medium ranging from  $3.16 \times 10^{-6}$  to  $1.3 \times 10^{-5}$  mol/m<sup>3</sup>-Pa for amorphous polyethylene to liquid benzene, respectively [55]. While the result of our analysis for  $k_D$  is in contrast with these base limits, it might be indicative of a transition in gas sorption mechanism upon coating hydration. Interestingly, the estimated  $k_D$  in Table 4 is close to, but slightly less than, the Henry's law constant for O<sub>2</sub> dissolution in liquid water at 65°C (i.e.,  $K_H = 0.0083$  mol/m<sup>3</sup>-Pa [28]). This reflects the effect of water vapor condensation inside the polymeric network and that the oxygen permeation was through sorption of gas in the mobile concentration of water inside FBE instead of independent O<sub>2</sub> transport through micropore sites. Indeed, new micropore sites evolved in the polymeric network with hydrothermal exposure [9], but because water molecules occupied these channels first, and because oxygen has a low solubility in the epoxy structure, the O<sub>2</sub> permeability in FBE took place through the dissolution of oxygen in the mobile concentration of water. The increase in immobilization factor of water ( $F_w$ ) compared to water vapor transport data (i.e., Table 2) also shows that the mobility of permeants in FBE microvoid channels can increase due to the increase in total feed pressure. Since the polymeric network is under plasticization by water, additional partial pressure of gas may induce break-up of water clusters within the coating membrane and result in a higher contribution of microvoid channels to diffusive transport. Importantly, the plasticization potential for mixed conditions is negative, indicating that water is limiting the diffusivity of O<sub>2</sub> through the polymeric network in FBE. This again supports the fact that the major pathway for transport of oxygen in the coating at 65°C was through the mobile concentration of water rather than dissolution in the polymeric phase. Also, the Langmuir affinity constant is higher than values normally identified for non-polar gases [36], [56]. However, at low pressure ranges, the individual

parameter  $b$  may not be regarded as very reliable (compared to  $C'_{Hb}$ ) [56] and thus it did not provide a valuable basis for transport analysis.

**Table 4**

Plasticization potential for water/oxygen mix ( $\beta'_{w-o_2}$ ), water immobilization factor ( $F_w$  based on water/oxygen data), the Henry's law constant for oxygen dissolution ( $k_{D,o_2}$ ), and the oxygen Langmuir affinity constant ( $b'_{o_2}$ ) for fusion bonded epoxy at 65°C, as determined from Eq. (12) and O<sub>2</sub> permeability data.

	$\beta'_{w-o_2}$	$F_w$	$k_{D,o_2}$	$b'_{o_2}$
	mol/m <sup>3</sup>	–	mol/m <sup>3</sup> -Pa	Pa <sup>-1</sup>
FBE at 65°C	-0.0053	0.89	0.0069	$2.66 \times 10^{-5}$

Our experimental and modeling analysis showed the predominant effect of service temperature on wet-state permeation of oxygen, in which solubility and transport of gaseous permeant in the polymeric network are highly competitive. As has been illustrated schematically in Fig. 8, transport of oxygen gas within the FBE coating at low temperatures ( $T < 65^\circ\text{C}$ ) experiences a blocking mechanism due to strong water clustering effects and high-chain stiffness. The Langmuir voids within the polymer (as key domains for gaseous dissolution) are occupied by water molecules and since free volume elements in glassy polymeric structures are not completely interconnected [8], the steady-state oxygen transport remains close to zero. On the other hand, when break-up of water clusters occurs upon increasing temperature, lower chain stiffness in epoxy network allows diffusion of oxygen molecules within the FBE structure and the resulting transport is primarily due to dissolution of gas molecules in mobile concentration of water. In addition, because cavity formation and cracking of polymeric network is a likely consequence of plasticization, the interconnectivity between Langmuir voids is increased which also favors the permeation of O<sub>2</sub>.



for FBE in Table 5 to provide a basis for comparing FBE and multilayered HPPC. Data for both coatings show that although the topcoat PE in HPPC does not play a key role in the barrier protection against gaseous transport, it improved the coating performance against plasticization of the FBE primer and induced a notable decline in O<sub>2</sub> ingress. Recall that the thickness of the primer FBE in HPPC was approximately half of a single layer FBE coating (i.e., 175-250 μm vs. 350-500μm, respectively). An explanation for the reduction in gas transport by the multilayered HPPC could be less availability of epoxy micropore sites for sorption in HPPC, compared to the direct exposure to humid feed gas in tests carried out on FBE.

**Table 5**

O<sub>2</sub> permeation results for fusion bonded epoxy and high-performance powder coating with respect to test temperatures, at water activity of 0.5 (i.e., equal water vapor saturation pressure and oxygen partial pressure in the feed volume).

Coating	Temperature (°C)	$P_{O_2} \times 10^{17}$ (mol/m-s-Pa)	Permeance $\times 10^{14}$ (mol/m <sup>2</sup> -s-Pa)
FBE	65	2.08 (± 1.08)	5.30 (±1.2)
FBE	70	1.82 (± 0.62)	3.45 (± 0.78)
FBE	80	1.77 (± 0.58)	4.00 (± 1.32)
HPPC	65	–	2.84 (± 1.42)
HPPC	70	–	2.34 (± 1.62)
HPPC	80	–	2.10 (± 0.66)

O<sub>2</sub> transport data for both coating systems in Table 5 were still about two orders of magnitude smaller than the minimum oxygen supply required for the underlying steel substrate corrosion. Upon hydration of the coating, the diffusion rate of O<sub>2</sub> is impeded (negative value of  $\beta'_{w-O_2}$  at 65°C), indicating pore filling effects and competitive sorption by water. Although the blocking mechanism for O<sub>2</sub> transport in powder coatings at elevated temperatures is sufficient to effectively halt corrosion, plasticization of the epoxy component is an important issue and significant changes in barrier performance are anticipated. Our experimental data for the membrane performance (i.e.,

Table 2 and 4) enable derivation of transport data for these coatings under a variety of humid feed gas conditions. However, we must note that permeability might depend on the evolving epoxy oxidation [57] and that accelerated polymer ageing under thermal oxidative conditions may also be a factor. Accordingly, the degradation process can manifest itself in consequences other than corrosion damage. Phenomena such as diffusion limited oxidation are heterogenous processes and can affect other barrier attributes of a coating structure such as adhesion [57]. Therefore, a performance assessment of FBE and HPPC when adhesion forces are present (as in coated pipelines) needs to be considered for coating characterization.

## 6. Conclusion

Water solubility, along with water clustering, plays a critical role in the dynamics of gas transport mechanism in FBE. Self-association of water molecules is a function of ageing time and temperature, which occurs at concentrations above half of the vapor saturation pressure (activity of 0.6 and above). If the temperature is less than 45°C, the glassy and stiff structure of FBE hinders the water-induced swelling mechanisms and only slight deviations from Henry's sorption are observed. At higher temperatures, however, water permeation exhibits a positive plasticization potential, meaning its diffusivity increases at higher concentrations. To find the water sorption parameters and plasticization potentials based on empirical data, we applied mathematical models proven for membrane gas separation to dense glassy FBE coating films. Our analysis of water vapor transport at 65°C showed that despite the restriction of diffusion caused by water clustering effects, nearly half of the microvoid regions in FBE ( $F_w = 0.49$ ) were involved in water transport. Possible explanations for this finding are cavity formation in the epoxy microstructure and break-up of water clusters at this temperature.

Under mixed feed conditions (water + oxygen), however, water tends to block O<sub>2</sub> transport in epoxy. At temperatures lower than 45°C, the associated immobilization was partial and the gas permeability decreased with increasing upstream gas pressure. Our time lag measurements in

wet-state conditions showed that O<sub>2</sub> ingress was several orders of magnitude lower than the amount required for cathodic reactions at the coating/metal substrate interface. Permeability values for oxygen transport in wet conditions at 25 and 40°C were less than 10<sup>-19</sup> mol/m-s-Pa (i.e., our detection limit). We used Freeman's upper bound theory to estimate the minimum O<sub>2</sub> ingress in the absence of plasticization effects, which again confirmed that a partial hydration of FBE (at well above 50% relative humidity) can cause remarkable oxygen deprivation for the under-coating corrosion reaction. In the multilayered HPPC, since water transport is effectively controlled by the topcoat PE component of the coating, the gas blocking effect evolves during gradual hydration of the FBE primer. This confirms that both coatings can support the corrosion protection of industrial infrastructure at service temperatures below 45°C in long-term ageing conditions. Our results show that unlike dry conditions in which oxygen permeation may not always be the rate determining step for under-coating corrosion reactions, the condensed water within epoxy in wet environments will reduce oxygen ingress by several orders of magnitude. Increasing temperature to 65°C (and above), water still acted as a blocking permeant for gas ingress, but transport of oxygen occurred through mobile concentration of water because of the reduction in chain-stiffness and gas selectivity. Our permeation analysis for 65°C showed the Henry's constant for oxygen dissolution in FBE under wet conditions was close to that of liquid water. This was an indicative of major role of water in gas sorption and transport in FBE in wet-state environments. Although water causes a partial blocking in oxygen transport throughout the epoxy network, break up of water clusters and low chain stiffness of the polymer facilitate the gas permeation through the mobile concentration of water. Our permeance data for these coatings showed that the multilayered HPPC outperforms the single layer FBE, despite having a thinner selective epoxy primer and that might be related to less availability of epoxy micropore sites in HPPC. Nevertheless, for an analytical assessment, one must note that corrosion damage might not be the only manifestation of coating degradation and other issues such as epoxy oxidation might affect the overall performance of the coating structure.

## Acknowledgment

The authors acknowledge funding support from the Natural Sciences and Engineering Research Council (NSERC) of Canada [NSERC CRDPJ 503725-16]. The funding and in-kind support from Shawcor Ltd. and Specialty Polymer Coatings Inc. [Industry portion - NSERC CRDPJ 503725-16] are also greatly appreciated.

## Appendix A

### A.1. Effect of temperature on the modified dual mode sorption parameters for epoxy systems

To find a model for explaining sigmoidal sorption isotherms in glassy polymers (e.g., water vapor/hydrophilic polymer systems), Feng employed statistical approaches to analyze interactions between sorbate molecules and sorption sites [25]. He divided the sorbed molecules into two groups: the monolayer molecules and multilayer molecules. The former correlates with the difference between the interaction of a microvoid and the first monolayer (measured with parameter  $A'$ ). The latter is a correction factor for the properties of the multilayer molecules relative to the bulk liquid, which demonstrates the departure of the sorption isotherm from linearity (denoted by  $k'$ ). Both of these parameters are assumed to follow an Arrhenius-type relation with temperature:

$$A' = A_0 \exp\left(\frac{H_m - H_n}{RT}\right) \quad (\text{A1})$$

$$k' = k_0 \exp\left(\frac{H_L - H_n}{RT}\right) \quad (\text{A2})$$

where  $A_0$  and  $k_0$  are pre-exponential factors;  $H_L$  is the heat of condensation of pure vapor (for water  $H_L = -40.7$  kJ/mol);  $H_m$  and  $H_n$  (in units of kJ/mol) are the heat of sorption of monolayer and multimolecular layers, respectively. Zhou and Lucas [53] classified water molecules in epoxy structures into two types: Type I with single hydrogen bonds that causes a transient decrease in glass transition temperature, and Type II that forms crosslinks and lessens the transient depression. The two sorption parameters defined in Eq. (A1) and (A2) are essentially equivalent

to Type I and II water molecules in epoxy resins [7].  $H_m$  represents the single layer Type I water molecules and  $H_n$  represents Type II molecules that form multi-site interconnective bonding [46]. In the modified DMS, there is not a strict Langmuir adsorption component compared to the original DMS model. Amounts of sorption in the matrix region and the microvoid region are functions of the weighted mean value of the sorption capacity of the polymer to the vapor ( $\overline{C_p}$ ). This parameter is a constant at a given temperature and depends on the structure and the state of the polymer [50]. To obtain the weighted sorption capacity for temperatures of interest in this study, we employed the Henry's law to involve the solubility and the concentration in terms of fugacity (i.e.,  $\overline{C_p} \propto S(T)f$ ). This assumption holds true since our focus is on a narrow temperature range (i.e., 50–80°C) and low pressures (less than 10 MPa). Accordingly, gas solubility in the polymer is likely to depend neither on the gas concentration, nor on the applied hydrostatic pressure [58]. Thus, we used the data for  $\overline{C_p}$  and  $S$  published by Lacombe et al. [39] and Bouvet et al. [52] (both from the same research group) on DGEBA/DAMP system, respectively.  $\overline{C_p}$  for different temperatures was obtained using the following equation:

$$\frac{\overline{C_p}^{-1}}{\overline{C_p}^{-2}} = \frac{S^1}{S^2} \times \frac{f_0^1}{f_0^2} \quad (\text{A3})$$

where  $f_0$  represents the saturated vapor fugacity and superscripts 1 and 2 denote variables evaluated at temperatures 1 and 2, respectively.

## References

- [1] G. Z. Xiao, M. Delamar, and M. E. R. Shanahan, "Irreversible interactions between water and DGEBA / DDA epoxy resin during hygrothermal aging," *J. Appl. Polym. Sci.*, vol. 65, no. 3, pp. 449–458, 1997, doi: [https://doi.org/10.1002/\(SICI\)1097-4628\(19970718\)65:3<449::AID-APP4>3.0.CO;2-H](https://doi.org/10.1002/(SICI)1097-4628(19970718)65:3<449::AID-APP4>3.0.CO;2-H).
- [2] C. A. Scholes, B. D. Freeman, and S. E. Kentish, "Water vapor permeability and competitive sorption in thermally rearranged (TR) membranes," *J. Memb. Sci.*, vol. 470, pp. 132–137, 2014, doi: 10.1016/j.memsci.2014.07.024.

- [3] B. D. Freeman, "Basis of permeability/selectivity tradeoff relations in polymeric gas separation membranes," *Macromolecules*, vol. 32, no. 2, pp. 375–380, 1999, doi: 10.1021/ma9814548.
- [4] L. M. Robeson, "The upper bound revisited," *J. Memb. Sci.*, vol. 320, no. 1–2, pp. 390–400, 2008, doi: 10.1016/j.memsci.2008.04.030.
- [5] M. M. Dal-Cin, A. Kumar, and L. Layton, "Revisiting the experimental and theoretical upper bounds of light pure gas selectivity-permeability for polymeric membranes," *J. Memb. Sci.*, vol. 323, no. 2, pp. 299–308, 2008, doi: 10.1016/j.memsci.2008.06.027.
- [6] A. Apicella, R. Tessieri, and C. de Cataldis, "Sorption modes of water in glassy epoxies," *J. Memb. Sci.*, vol. 18, no. C, pp. 211–225, 1984, doi: 10.1016/S0376-7388(00)85035-8.
- [7] H. Zargarneshad, E. Asselin, D. Wong, and C. Lam, "A critical review of the time-dependent performance of polymeric pipeline coatings: Focus on hydration of epoxy-based coatings," *Polymers (Basel)*, vol. 13, no. 9, p. 1517, 2021, doi: 10.3390/polym13091517.
- [8] M. Minelli and G. C. Sarti, "Permeability and diffusivity of CO<sub>2</sub> in glassy polymers with and without plasticization," *J. Memb. Sci.*, vol. 435, pp. 176–185, 2013, doi: 10.1016/j.memsci.2013.02.013.
- [9] H. Zargarneshad, E. Asselin, D. Wong, and C. N. C. Lam, "Water transport through epoxy-based powder pipeline coatings," *Prog. Org. Coatings*, vol. 168, no. March, p. 106874, 2022, doi: 10.1016/j.porgcoat.2022.106874.
- [10] W. Funke and H. Haagen, "Empirical or Scientific Approach to Evaluate the Corrosion Protective Performance of Organic Coatings," *Ind. Eng. Chem. Prod. Res. Dev.*, vol. 17, no. 1, pp. 50–53, 1978, doi: 10.1021/i360065a014.
- [11] N. S. Sangaj and V. C. Malshe, "Permeability of polymers in protective organic coatings," *Prog. Org. Coatings*, vol. 50, no. 1, pp. 28–39, 2004, doi: 10.1016/j.porgcoat.2003.09.015.
- [12] M. C. Celina and A. Quintana, "Oxygen diffusivity and permeation through polymers at elevated temperature," *Polymer (Guildf)*, vol. 150, pp. 326–342, 2018, doi:

10.1016/j.polymer.2018.06.047.

- [13] C. N. C. Lam, D. T. Wong, R. E. Steele, and S. J. Edmondson, "A new approach to high performance polyolefin coatings," in Corrosion Conference and Expo, 2007, no. 07023.
- [14] S. W. Guan, K. Y. Chen, N. Uppal, S. McLennan, and P. Mayes, "A novel anti-corrosion pipeline coating solution," *Annu. Conf. Australas. Corros. Assoc. 2014 Corros. Prev.* 2014, pp. 1–9, 2014.
- [15] M. Mobin et al., "Performance evaluation of some fusion-bonded epoxy coatings under water transmission line conditions," *Prog. Org. Coatings*, vol. 62, no. 4, pp. 369–375, 2008, doi: 10.1016/j.porgcoat.2008.02.002.
- [16] C. Khoe, S. Chowdhury, V. R. Bhethanabotla, and R. Sen, "Measurement of oxygen permeability of epoxy polymers," *ACI Mater. J.*, vol. 107, no. 2, pp. 138–146, 2010, doi: 10.14359/51663577.
- [17] M. Romano et al., *Protecting and maintaining transmission pipeline*. Pittsburgh, PA, 2012.
- [18] K. Nakamura et al., "Permeability of dry gases and those dissolved in water through hydrophobic high free-volume silicon- or fluorine-containing nonporous glassy polymer membranes," *Ind. Eng. Chem. Res.*, vol. 52, no. 3, pp. 1133–1140, 2013, doi: 10.1021/ie300793t.
- [19] C. A. Scholes, S. Kanehashi, G. W. Stevens, and S. E. Kentish, "Water permeability and competitive permeation with CO<sub>2</sub> and CH<sub>4</sub> in perfluorinated polymeric membranes," *Sep. Purif. Technol.*, vol. 147, pp. 203–209, 2015, doi: 10.1016/j.seppur.2015.04.023.
- [20] P. A. Saliba, A. A. Mansur, D. B. Santos, and H. S. Mansur, "Fusion-bonded epoxy composite coatings on chemically functionalized API steel surfaces for potential deep-water petroleum exploration," *Appl. Adhes. Sci.*, vol. 3, no. 1, 2015, doi: 10.1186/s40563-015-0052-2.
- [21] P. A. Saliba, A. A. P. Mansur, and H. S. Mansur, "Advanced Nanocomposite Coatings of Fusion Bonded Epoxy Reinforced with Amino-Functionalized Nanoparticles for Applications in Underwater Oil Pipelines," *J. Nanomater.*, vol. 2016, 2016, doi:

10.1155/2016/7281726.

- [22] E. Legghe, E. Aragon, L. Bélec, A. Margailan, and D. Melot, "Correlation between water diffusion and adhesion loss: Study of an epoxy primer on steel," *Prog. Org. Coatings*, vol. 66, no. 3, pp. 276–280, 2009, doi: 10.1016/j.porgcoat.2009.08.001.
- [23] ASTM, Standard Test Method for Nondestructive Measurement of Dry Film Thickness of Applied Organic Coatings Using an Ultrasonic Gage (ASTM D 6132), no. Reapproved 2017. West Conshohocken, 2017, pp. 8–10.
- [24] T. C. Merkel, V. Bondar, K. Nagai, and B. D. Freeman, "Hydrocarbon and perfluorocarbon gas sorption in poly(dimethylsiloxane), poly(1-trimethylsilyl-1-propyne), and copolymers of tetrafluoroethylene and 2,2-bis(trifluoromethyl)-4,5-difluoro-1,3-dioxole," *Macromolecules*, vol. 32, no. 2, pp. 370–374, 1999, doi: 10.1021/ma9814402.
- [25] H. Feng, "Modeling of vapor sorption in glassy polymers using a new dual mode sorption model based on multilayer sorption theory," *Polymer (Guildf)*, vol. 48, no. 10, pp. 2988–3002, 2007, doi: 10.1016/j.polymer.2006.10.050.
- [26] G. Q. Chen, C. A. Scholes, G. G. Qiao, and S. E. Kentish, "Water vapor permeation in polyimide membranes," *J. Memb. Sci.*, vol. 379, no. 1–2, pp. 479–487, 2011, doi: 10.1016/j.memsci.2011.06.023.
- [27] H. Zargarneshad, E. Asselin, D. Wong, and C. Lam, "Oxygen permeability of powder-based coatings in wet diffusion systems," 2020.
- [28] D. Tromans, "Temperature and pressure dependent solubility of oxygen in water: A thermodynamic analysis," *Hydrometallurgy*, vol. 48, no. 3, pp. 327–342, 1998, doi: 10.1016/s0304-386x(98)00007-3.
- [29] R. J. Varley and K. H. Leong, "Polymer Coatings for Oilfield Pipelines," in *Active Protective Coatings: New-Generation Coatings for Metals*, A. E. Hughes, J. M. C. Mol, M. L. Zheludkevich, and R. G. Buchheit, Eds. Dordrecht, Netherlands: Springer, 2016, pp. 385–428.
- [30] L. M. Robeson, "Correlation of separation factor versus permeability for polymeric

- membranes," *J. Memb. Sci.*, vol. 62, no. 2, pp. 165–185, 1991, doi: 10.1016/0376-7388(91)80060-J.
- [31] L. M. Robeson, Z. P. Smith, B. D. Freeman, and D. R. Paul, "Contributions of diffusion and solubility selectivity to the upper bound analysis for glassy gas separation membranes," *J. Memb. Sci.*, vol. 453, pp. 71–83, 2014, doi: 10.1016/j.memsci.2013.10.066.
- [32] E. M. Davis and Y. A. Elabd, "Water clustering in glassy polymers," *J. Phys. Chem. B*, vol. 117, no. 36, pp. 10629–10640, 2013, doi: 10.1021/jp405388d.
- [33] W. Xie, J. Cook, H. B. Park, B. D. Freeman, C. H. Lee, and J. E. McGrath, "Fundamental salt and water transport properties in directly copolymerized disulfonated poly(arylene ether sulfone) random copolymers," *Polymer (Guildf)*, vol. 52, no. 9, pp. 2032–2043, 2011, doi: 10.1016/j.polymer.2011.02.006.
- [34] J. E. Robertson, T. C. Ward, and A. J. Hill, "Thermal, mechanical, physical, and transport properties of blends of novel oligomer and thermoplastic polysulfone," *Polymer (Guildf)*, vol. 41, no. 16, pp. 6251–6262, 2000, doi: 10.1016/S0032-3861(99)00829-0.
- [35] M. Minelli, S. Oradei, M. Fiorini, and G. C. Sarti, "CO<sub>2</sub> plasticization effect on glassy polymeric membranes," *Polymer (Guildf)*, vol. 163, no. December 2018, pp. 29–35, 2019, doi: 10.1016/j.polymer.2018.12.043.
- [36] C. A. Scholes, J. Jin, G. W. Stevens, and S. E. Kentish, "Competitive permeation of gas and water vapour in high free volume polymeric membranes," *J. Polym. Sci. Part B Polym. Phys.*, vol. 53, no. 10, pp. 719–728, 2015, doi: 10.1002/polb.23689.
- [37] M. Minelli and G. C. Sarti, "Gas permeability in glassy polymers: A thermodynamic approach," *Fluid Phase Equilib.*, vol. 424, pp. 44–51, 2016, doi: 10.1016/j.fluid.2015.09.027.
- [38] D. R. Paul, W. J. Koros, and C. Engineering, "Effect of partially immobilizing sorption on permeability and the diffusion time lag," *J. Polym. Sci. Polym. Phys. Ed.*, vol. 14, pp. 675–685, 1976, doi: <https://doi.org/10.1002/pol.1976.180140409>.

- [39] C. Vosgien Lacombe, G. Bouvet, D. Trinh, X. Feaugas, S. Touzain, and S. Mallarino, "Influence of pigment and internal stresses on water uptake in model epoxy: a thermodynamic approach," *J. Mater. Sci.*, vol. 53, no. 3, pp. 2253–2267, 2018, doi: 10.1007/s10853-017-1647-8.
- [40] G. Q. Chen, C. A. Scholes, C. M. Doherty, A. J. Hill, G. G. Qiao, and S. E. Kentish, "Modeling of the sorption and transport properties of water vapor in polyimide membranes," *J. Memb. Sci.*, vol. 409–410, pp. 96–104, 2012, doi: 10.1016/j.memsci.2012.03.047.
- [41] X. Duthie, S. Kentish, C. Powell, K. Nagai, G. Qiao, and G. Stevens, "Operating temperature effects on the plasticization of polyimide gas separation membranes," *J. Memb. Sci.*, vol. 294, no. 1–2, pp. 40–49, 2007, doi: 10.1016/j.memsci.2007.02.004.
- [42] S. Sato, M. Suzuki, S. Kanehashi, and K. Nagai, "Permeability, diffusivity, and solubility of benzene vapor and water vapor in high free volume silicon- or fluorine-containing polymer membranes," *J. Memb. Sci.*, vol. 360, no. 1–2, pp. 352–362, 2010, doi: 10.1016/j.memsci.2010.05.029.
- [43] C. A. Scholes, J. Jin, G. W. Stevens, and S. E. Kentish, "Hydrocarbon solubility, permeability, and competitive sorption effects in polymer of intrinsic microporosity (PIM-1) membranes," *J. Polym. Sci. Part B Polym. Phys.*, vol. 54, no. 3, pp. 397–404, 2016, doi: 10.1002/polb.23900.
- [44] G. Bouvet, N. Dang, S. Cohendoz, X. Feaugas, S. Mallarino, and S. Touzain, "Impact of polar groups concentration and free volume on water sorption in model epoxy free films and coatings," *Prog. Org. Coatings*, vol. 96, pp. 32–41, 2016, doi: 10.1016/j.porgcoat.2015.12.011.
- [45] C. Carfagna and A. Apicella, "Physical degradation by water clustering in epoxy resins," *J. Appl. Polym. Sci.*, vol. 28, pp. 2881–2885, 1983, doi: <https://doi.org/10.1002/app.1983.070280917>.
- [46] J. Zhou and J. P. Lucas, "Hygrothermal effects of epoxy resin. Part I: the nature of water

- in epoxy,” *Polymer (Guildf)*., vol. 40, no. 20, pp. 5505–5512, 1999, doi: 10.1016/S0032-3861(98)00790-3.
- [47] Y. Ding, M. Liu, S. Li, S. Zhang, W.-F. Zhou, and B. Wang, “Contributions of the Side Groups to the Characteristics of Water Absorption in Cured Epoxy Resins,” *Mol. Chem. Phys.*, vol. 202, no. 13, pp. 2681–2685, 2001.
- [48] A. D. Drozdov, J. De, R. K. Gupta, and A. P. Shah, “Model for anomalous moisture diffusion through a polymer-clay nanocomposite,” *J. Polym. Sci. Part B Polym. Phys.*, vol. 41, no. 5, pp. 476–492, 2003, doi: <https://onlinelibrary.wiley.com/doi/10.1002/polb.10393>.
- [49] A. Quintana and M. C. Celina, “Overview of DLO modeling and approaches to predict heterogeneous oxidative polymer degradation,” *Polym. Degrad. Stab.*, vol. 149, pp. 173–191, 2018, doi: 10.1016/j.polymdegradstab.2017.11.014.
- [50] S. Kanehashi and K. Nagai, “Analysis of dual-mode model parameters for gas sorption in glassy polymers,” *J. Memb. Sci.*, vol. 253, no. 1–2, pp. 117–138, 2005, doi: 10.1016/j.memsci.2005.01.003.
- [51] M. C. Celina, A. R. Dayile, and A. Quintana, “A perspective on the inherent oxidation sensitivity of epoxy materials,” *Polymer (Guildf)*., vol. 54, no. 13, pp. 3290–3296, 2013, doi: 10.1016/j.polymer.2013.04.042.
- [52] G. Bouvet, S. Cohendoz, X. Feaugas, S. Touzain, and S. Mallarino, “Microstructural reorganization in model epoxy network during cyclic hygrothermal ageing,” *Polymer (Guildf)*., vol. 122, pp. 1–11, 2017, doi: 10.1016/j.polymer.2017.06.032.
- [53] M. S. Delaney, D. Reddy, and R. A. Wessling, “Oxygen/nitrogen transport in glassy polymers with oxygen-binding pendent groups,” *J. Memb. Sci.*, vol. 49, no. 1, pp. 15–36, 1990, doi: 10.1016/S0376-7388(00)80775-9.
- [54] C. A. Scholes, W. X. Tao, G. W. Stevens, and S. E. Kentish, “Sorption of Methane, Nitrogen, Carbon Dioxide, and Water in Matrimid 5218,” *J. Appl. Polym. Sci.*, vol. 117, no. 4, pp. 2284–2289, 2010, doi: 10.1002/app.
- [55] K. Toi, G. Morel, and D. R. Paul, “Gas sorption and transport in poly(phenylene oxide) and

comparisons with other glassy polymers,” *J. Appl. Polym. Sci.*, vol. 27, no. 8, pp. 2997–3005, 1982, doi: 10.1002/app.1982.070270823.

- [56] A. J. Erb and D. R. Paul, “Gas Sorption and Transport in polysulfone,” *J. Memb. Sci.*, vol. 8, pp. 11–22, 1981.
- [57] A. Quintana and M. C. Celina, “Overview of DLO modeling and approaches to predict heterogeneous oxidative polymer degradation,” *Polym. Degrad. Stab.*, vol. 149, no. November, pp. 173–191, 2018, doi: 10.1016/j.polymdegradstab.2017.11.014.
- [58] M. H. Klopffer and B. Flaconnèche, “Transport Properties of Gases in Polymers : Bibliographic Review,” *Oil Gas Sci. Technol.*, vol. 56, no. 3, pp. 223–244, 2001.